

Article

# Isolation and Characterization of Two Microalgal Isolates from Vietnam with Potential for Food, Feed, and Biodiesel Production

Thao Nguyen Luu <sup>1,2</sup> , Zouheir Alsafr <sup>3</sup>, Amélie Corato <sup>4</sup>, Daniele Corsaro <sup>5</sup>, Hung Anh Le <sup>6</sup>, Gauthier Eppe <sup>3,\*</sup>  and Claire Remacle <sup>1,\*</sup>

<sup>1</sup> Genetics and Physiology of Microalgae, InBios/Phytosystems Research Unit, University of Liege, 4000 Liege, Belgium; luuthaonguyen@iuh.edu.vn

<sup>2</sup> Institute of Biotechnology and Food Technology, Industrial University of Ho Chi minh City, 71406 Ho Chi minh, Vietnam

<sup>3</sup> Laboratory of Mass Spectrometry, MolSys Research Unit, University of Liege, 4000 Liege, Belgium; zouheir.alsafr@doct.ulg.ac.be

<sup>4</sup> Bioenergetics, InBios/Phytosystems Research Unit, University of Liege, 4000 Liege, Belgium; Amelie.Corato@uliege.be

<sup>5</sup> CHLAREAS, 12, rue du Maconnais, F-54500 Vandoeuvre-lès-Nancy, France; corsaro@gmx.fr

<sup>6</sup> Institute of Environmental Science, Engineering and Management, Industrial University of Ho Chi minh City, 71406 Ho Chi minh, Vietnam; lehunganh@iuh.edu.vn

\* Correspondence: g.eppe@uliege.be (G.E.); c.remacle@uliege.be (C.R.); Tel.: +32-366-34-22 (G.E.); +32-366-38-12 (C.R.)

Received: 29 December 2019; Accepted: 11 February 2020; Published: 18 February 2020



**Abstract:** Microalgae are promising feedstock for the production of biodiesel and diverse medium- and high-value products such as pigments and polyunsaturated fatty acids. The importance of strain selection adapted to specific environments is important for economical purposes. We characterize here two microalgal strains, isolated from wastewater of shrimp cultivation ponds in Vietnam. Based on the 18S rDNA-ITS region, one strain belongs to the Eustigmatophyceae class and is identical to the *Nannochloropsis salina* isolate D12 (JX185299.1), while the other is a Chlorophyceae belonging to the *Desmodesmus* genus, which possesses a S516 group I intron in its 18S rDNA gene. The *N. salina* strain is a marine and oleaginous microalga (40% of dry weight (DW) at stationary phase) whole oil is rich in saturated fatty acids (around 45% of C16:0) suitable for biodiesel and contains a few percent of eicosapentaenoic acid (C20:5). The *Desmodesmus* isolate can assimilate acetate and ammonium and is rich in lutein. Its oil contains around 40%–50%  $\alpha$ -linolenic acid (C18:3), an essential fatty acid. Since they tolerate various salinities (10% to 35‰), both strains are thus interesting for biodiesel or aquaculture valorization in coastal and tropical climate where water, nutrient, and salinity availability vary greatly depending on the season.

**Keywords:** microalga; fatty acid; Vietnam; *Nannochloropsis*; *Desmodesmus*

## 1. Introduction

Microalgae are phototrophic organisms representing a promising feedstock for the production of biodiesel and diverse medium- and high-value products [1]. They can live in various habitats, including freshwater, brackish water, and marine environments such as oceans, lagoons, and ponds where the salinity can be subject to fluctuations due to drought or heavy rains in tropical climates. The importance of strain selection for economically viable algal-based bioproducts is recognized [2] and the selection should focus on different criteria such as the capacity to accumulate large amounts

of the desired compound or to grow in specific conditions (salt tolerance, temperature, etc.) [2]. In addition, utilization of the whole microalgal biomass is desirable to increase the chances of commercial success. In this context, coupling production of value-added bioproducts with microalgal biofuel has been suggested to be a promising technology to reduce costs [3].

Medium- and high-value products include long chain polyunsaturated fatty acids (PUFAs) and carotenoids.  $\omega$ -3 PUFAs [eicosapentaenoic acid (EPA C20:5n-3) and docosapentaenoic acid (DHA C22:6n-3)] have nutritive values important for aquaculture and for human health [4,5]. Nowadays, EPA and DHA are mainly found in fish oil, but overfishing has reduced wild fish stocks [6]. Thus, industries look for additional sources of natural EPA and DHA and microalgae that contain substantial amount of  $\omega$ -3 PUFAs seem to be interesting. Carotenoids are pigments that are found important as they protect cells from oxidative damage. They represent food and feed additives and health-promoting supplements [7]. Microalgae containing substantial amounts of pigments such as  $\beta$ -carotene, lutein, canthaxanthin, astaxanthin, phycocyanin, and fucoxanthin are thus commercially interesting [4,8].

With the aim to find strains suitable for growth in tropical climate and adapted to changing salinity environment, we have isolated two microalgae from wastewater of shrimp cultivation ponds located in the coastal region of the Ninh Thuan province, Vietnam. The two strains were identified based on the 18S rDNA-ITS region. One strain belongs to the Eustigmatophyceae class and is identical to the *Nannochloropsis salina* isolate D12 (JX185299.1) recorded in GenBank while the other is a Chlorophyceae belonging to the *Desmodesmus* genus. They are part of distant phyla. *Desmodesmus* belongs to Chlorophyta characterized by chloroplasts derived from primary endosymbiosis with a cyanobacterium whose most probable living counterpart is the fresh water-dwelling *Gloeomargarita lithophora*. *Nannochloropsis* belongs to Stramenopiles characterized by chloroplasts derived from a secondary symbiosis event with a red alga [9–12]. Characterization of both strains is performed in terms of growth, protein content, fatty acid, pigment profile, and resistance to salinity stress in order to assess their potential for biotechnological applications in this region.

## 2. Materials and Methods

### 2.1. Isolation and Purification of Microalgae

Marine water samples were collected from shrimp cultivation ponds at Marine seed center at level I, Ninh Thuan province, Vietnam (Latitude 11°30'33.4" N—Longitude 109°00'35.6" E) and first enriched in the laboratory using liquid F/2 medium with salinity of 24‰. The enrichment culture was aerated using an orbital shaker. The growth was maintained at  $35 \pm 1$  °C under constant illumination. After 2 weeks, 100  $\mu$ L of greenish enrichment cultures were spread on plate of solid F/2 medium (salinity of 24‰) containing 1.5% agar and ampicillin (0.1  $\mu$ g mL<sup>-1</sup>). Ampicillin was used to eliminate the bacterial contaminants. The solid plates were incubated under constant illumination at  $22 \pm 1$  °C until microalgal colonies along with bacterial and fungal colonies appeared on plates. Streak plate technique was repeated until the axenic cultures were obtained. To ensure the axenicity of isolates, light microscope and lab binocular were used to observe the algal cells and colonies, respectively.

### 2.2. DNA Isolation, PCR and DNA Sequencing

DNA isolation was performed according to [13]. The 18S rDNA-ITS sequence of isolates *nl3* and *nl6* was amplified using primers NS1 and ITS4 with standard PCR protocol and the PCR product was sequenced using these two primers, as well as the internal primers NS2, NS3, NL4, NS5, NS8, and ITS1 (Beckman Coulter Company, Takeley, UK).

The overlapping partial sequences between two consecutive sequences were assembled using NCBI Blast Tool (Standard nucleotide blast) to obtain a complete 18S rDNA-ITS1-5.8S-ITS2 sequence which was compared with sequences on NCBI database for hits. The sequence of *nl3* is deposited in GenBank (MN746324).

### 2.3. Microalgal Growth

Isolate *nl3* and *nl6* were cultivated in 250 mL Erlenmeyer flasks containing sterile TAP (Tris-Acetate-Phosphate) medium [14] or Guillard's F/2 medium (Sigma-Aldrich, St Louis, MO, USA) [15] with salinity ranging between 0–35‰ when specified. Cultures were aerated on a shaker and continuously illuminated with constant illumination of  $200 \mu\text{mol m}^{-2}\text{s}^{-1}$  at  $25 \pm 1$  °C. The optical density at wavelength of 750 nm was measured every day to evaluate the cell density [16] using three biological replicates. The data were expressed as mean  $\pm$  standard deviation ( $\pm$ SD).

$$\mu = (\ln N - \ln N_0)/(t - t_0) \quad (1)$$

The specific growth rate ( $\mu$ ) was calculated using Formula (1) [17] in which  $N_0$  and  $N$  stand for the  $OD_{750}$  value at the beginning ( $t_0$ ) and the end of exponential phase ( $t$ ), respectively.

### 2.4. Biomass Analysis

#### 2.4.1. Dry Weight

40 mL of culture was harvested in a falcon tube. The tube was centrifuged at 1500 g for 10 min. The supernatant was discarded. Three mL of distilled water were added to the pellet and transferred to a pre-weighed glass tube. The glass tube was centrifuged at 800 g for 10 min to remove the supernatant. The glass tube containing wet biomass was allowed to dry in oven at 80 °C until constant weight was achieved. Three biological triplicates were used. The data were expressed as mean  $\pm$  standard deviation ( $\pm$ SD).

#### 2.4.2. Fatty Acid Methyl Ester Analysis (FAME) Analysis

FAME preparation was carried out using a process involving two main steps: lipid extraction and transesterification. Two to ten mL aliquot of each algal culture was harvested in a falcon tube and centrifuged for 10 min at  $4000 \times g$ , 4 °C. Two mL of Folch reagent (Chloroform–Methanol) were added to the pellet. The suspension was sonicated in an ice bath for 10 min to break the cell wall. One mL of the cell/Folch mixture was transferred to a sterile glass tube using Pasteur pipette. Thirty  $\mu\text{L}$  of internal standard C15:0 were added to the tube using a Hamilton syringe prior to transesterification reaction. The mixture was evaporated to dryness at 80 °C. One mL of  $\text{BF}_3/\text{Methanol}$  (Sigma-Aldrich, St Louis, MO, USA), was added in the tube, sealed and homogenized. The mixture was heated at 95 °C for 10 min in a water bath to conduct transesterification reaction. The reaction tube was slowly cooled down to room temperature within 15–20 min. One mL of water and 1 mL of hexane were added and the reaction tube was stirred for 30 min on a carousel. A centrifugation at  $200 \times g$  for 10 min, 4 °C was then conducted. The lower aqueous phase was eliminated from the tube using a Pasteur pipette. Again, 1 mL of ultra-pure water was poured in the tube, mixed, and centrifuged for 10 min at  $200 \times g$ , 4 °C. The tube was stored in the freezer overnight. The organic phase (top phase) containing FAMES was transferred to a two-milliliter chromacol vial, hermetically sealed with a cap and stored at -20 °C until analysis.

FAME analyses were conducted on a Trace GC2000-PolarisQ ion trap mass spectrometer (ThermoScientific, Waltham, MA, USA) coupled with CTC Combi-Pal autosampler (CTC Analytics, Zwingen, Switzerland). FAMES were separated in GC column SP2331 (30 m  $\times$  0.25 mm ID  $\times$  0.20  $\mu\text{m}$  film thickness, Supelco, Bellefonte, PA, USA). with helium as carrier gas. The GC temperature program consisted of 4 thermal steps; the column was initially held at 60 °C for 2 min; then ramped to 180 °C at a rate of 5 °C  $\text{min}^{-1}$ ; followed by a rate of 10 °C  $\text{min}^{-1}$  to 250 °C maintained during 1 min. Mass spectral profile, comparison to external standards and retention time were criteria used to identify FAMES. Quantification of FAMES was done using calibration curves of FAME external standards and C15:0 internal standard. Three biological triplicates were used unless otherwise stated, and the data were expressed as mean  $\pm$  standard deviation ( $\pm$ SD).

### 2.4.3. Biodiesel Fuel Properties Based on FAME Profiles

Some properties of biodiesel were calculated using the following equations [18]

$$\text{Average degree of unsaturation (ADU)} = \sum A \times k$$

A: % of each fatty acid on total fatty acids; k: number of double bonds in each fatty acid  
Kinematic viscosity =  $-0.6316 \times \text{ADU} + 5.2065$  (kV) ( $\text{mm}^2 \cdot \text{s}^{-1}$ ).

$$\text{Kinematic viscosity (kV)} = -0.6316 \times \text{ADU} + 5.2065 \text{ (mm}^2 \text{ s}^{-1}\text{)}$$

$$\text{Specific gravity (SG)} = 0.0055 \times \text{ADU} + 0.8726 \text{ (kg L}^{-1}\text{)}$$

$$\text{Cloud point (CP)} = -13.356 \times \text{ADU} + 19.994 \text{ (}^\circ\text{C)}$$

$$\text{Cetane number (CN)} = -6.6684 \times \text{ADU} + 62.876$$

$$\text{Iodine value (IV)} = 74.373 \times \text{ADU} + 12.71 \text{ (gI}_2 \text{ 100 g}^{-1}\text{)}$$

$$\text{Higher heating value (HHV)} = 1.7601 \times \text{ADU} + 38.534 \text{ (Mj kg}^{-1}\text{)}$$

### 2.4.4. Protein Content

1 mL of culture was harvested for protein assay. The pellet containing wet biomass was suspended in 1 mL 50 mM HEPES-KOH pH 7.2 and 5  $\mu\text{L}$  phenylmethanesulfonyl fluoride (PMSF) 100  $\mu\text{M}$ . About 600 mg of glass beads (0.5 mm) were added to the tube and vortexed for 40 min at maximum level, 4  $^\circ\text{C}$ . A 20  $\mu\text{L}$  aliquot of the extract was used for Bradford assay [19]. The sample volume was brought to 100  $\mu\text{L}$  with buffer solution (0.1 M NaOH, 0.1% Triton). The sample was mixed with 1 mL of Bradford reagent (1X). Dye will bind to protein to have a blue protein-dye form. Optical absorbance of mixture was read by PDA UV/VIS Lambda 265 Spectrophotometer (PerkinElmer, Waltham, MA, USA) at 595 nm. The concentration of protein in sample was presented as  $\mu\text{g/mL}$  and calculated based on the standard curve using optical absorbance against bovine serum albumin (BSA) concentration. Three biological triplicates were used unless otherwise stated. The data were expressed as mean  $\pm$  standard deviation ( $\pm\text{SD}$ ).

### 2.4.5. Pigment Analysis

1 mL of culture was harvested to collect the biomass at 4  $^\circ\text{C}$ . Pigments were extracted in 1 mL  $\text{CH}_2\text{Cl}_2:\text{CH}_3\text{OH}$  (1:3) using glass beads of 0.5 mm at 4  $^\circ\text{C}$  for 40 min. The supernatant was collected by centrifugation at 20,000 $\times g$  for 15 min and filtered through 0.2  $\mu\text{m}$  pores before loading into HPLC system. The HPLC device was a Shimadzu equipped with a photodiode array detector DAD (SPD-M20A). The pigment separation was conducted in reverse phase gradient mode with a CORTECS C18 column (90  $\text{\AA}$  pore size, 2.7  $\mu\text{m}$  solid-core particles, 4.6 mm  $\times$  150 mm, 3/pk, Waters), under a flow of 1 mL  $\text{min}^{-1}$ , at 25  $^\circ\text{C}$ . The solvents used were  $\text{NH}_4\text{Ac}$  50 mM + 75% Acetonitrile (A), 90% Acetonitrile (B) and Ethyl Acetate (100%) (C), and the gradient was 0 min—100% A; 2.5 min—100% B; 3.1 min—90% B + 10% C; 8.1 min—65% B + 35% C; 13.5 min—40% B + 60% C; 17 min—100% C; 19 min—100% A; 25 min—100% A. The quantification was based on peaks areas at 430 nm in comparison with an external standard (DHI Lab Products).

### 2.5. Intron Analysis

The secondary structure of the intron was deduced, first by identifying the conserved pairs P3–P7, then by deducing with Mfold the remaining parts, using as a guide a set of sequences and structures previously established. For phylogenetic analysis, class E introns present in nuclear rDNA of closely related algae as well as of distant species, were selected. A set of class C introns has also been selected and used as outgroup. The sequences were aligned according to the secondary structure considering only the conserved P3–P8 core, and the tree was constructed with Maximum Likelihood (ML, GTR +  $\Gamma$ ; 1000 bootstraps), as previously described [20,21].

## 2.6. 18S rDNA Phylogeny

For identification, sequence of 18S rDNA excluding the introns and complete ITS1-5.8S-ITS2 region of isolate *nl3* was searched against non-redundant nucleotide database for homologous sequences using online blast program (BLASTN) (<http://www.ncbi.nlm.nih.gov/BLAST/>). Clustal X2.1 software was then employed for the automatic multiple alignments of homologous sequences and studied sequence. A preliminary analysis with Paup was carried out [22]. Phylogenetic trees were generated using maximum likelihood (ML, GTR, G + I:4 model) with TREEFINDER [23], distance (neighbour-joining, K2 model) and maximum parsimony (MP) with MEGA7 [24]), with 1000 bootstraps.

## 3. Results

### 3.1. Sequencing of the rDNA-ITS Region

A PCR fragment was obtained using the primers NS1 and ITS4 (Table 1) for both strains named *nl3* and *nl6*. These primers, originally described to amplify the 18S-ITS1-5.8S-ITS2 rDNA region in fungi [25], proved also to work well for land plants [26]. The PCR fragment has a size of around 3500 bp for *nl3* and 2600 bp for *nl6*. PCR products were sequenced using the primers listed in Table 1 in both forward and reverse orientations and blasted against the sequences deposited on NCBI database. The BLAST search results showed for *nl6* a 100% identity with *N. salina* (D12, accession number JX185299.1), while *nl3* proved to be closer although not identical to *Desmodesmus* sp. GM4i (AB917136.1). The sequence of *Desmodesmus* sp. *nl3* is deposited in GenBank (MN746324). *Desmodesmus* sp. *nl3* and *Desmodesmus* sp. GM4i, both have an intron inserted at the same position in the 18S rDNA, S516 (referring to the insertion in the rDNA of *E. coli*), although the *nl3* is longer in size (754 pb versus 404 bp). The presence of S516 intron in *Desmodesmus* GM4i has already been reported [27]. Therefore, we analyzed the secondary structure of the *nl3* S516 intron. It comprises the 9 typical stem-loop structures of group I introns, with an additional loop of 347 bp at the level of the P9.3 branch (Figure 1). Overall, the deduced structure and sequence variations strongly indicate that the intron belongs to the E class [28], probably of the E2 type. Another group I intron, S1046, class C, is also present in the 18S rDNA of the strain *nl3*.

**Table 1.** Primers used in this study.

Primer	Sequence (5'-3')	DNA Region Amplified
NS1	GTAGTCATATGCTTGCTC	SSU
NS2	GGCTGCTGGCACCAGACTTGC	SSU
NS3	GCAAGTCTGGTGCCAGCAGCC	SSU
NS4	CTCCGTC AATTCCTTTAAG	SSU
NS5	AACTTAAAGGAATTGACGGAAG	SSU
NS8	TCCGCAGGTTACCTACGGA	SSU
ITS1	TCCGTAGGTGAACCTGCGG	ITS1
ITS3	GCATCGATGAAGAACGCAGC	ITS2
ITS4	TCCTCCGCTTATTGATATGC	ITS2

### 3.2. Phylogenetic Analysis of the *nl3* Sequence

In order to position *nl3* at the molecular level, phylogenetic analyses were performed using a set of selected microalgal rDNAs including some closely related sequences where introns present were excluded. The results show that isolate *nl3* branches with two strains of *Desmodesmus subspicatus* (Figure 2). Therefore, isolate *nl3* is a green microalgal species, belonging to the genus *Desmodesmus*, family Scenedesmaceae.

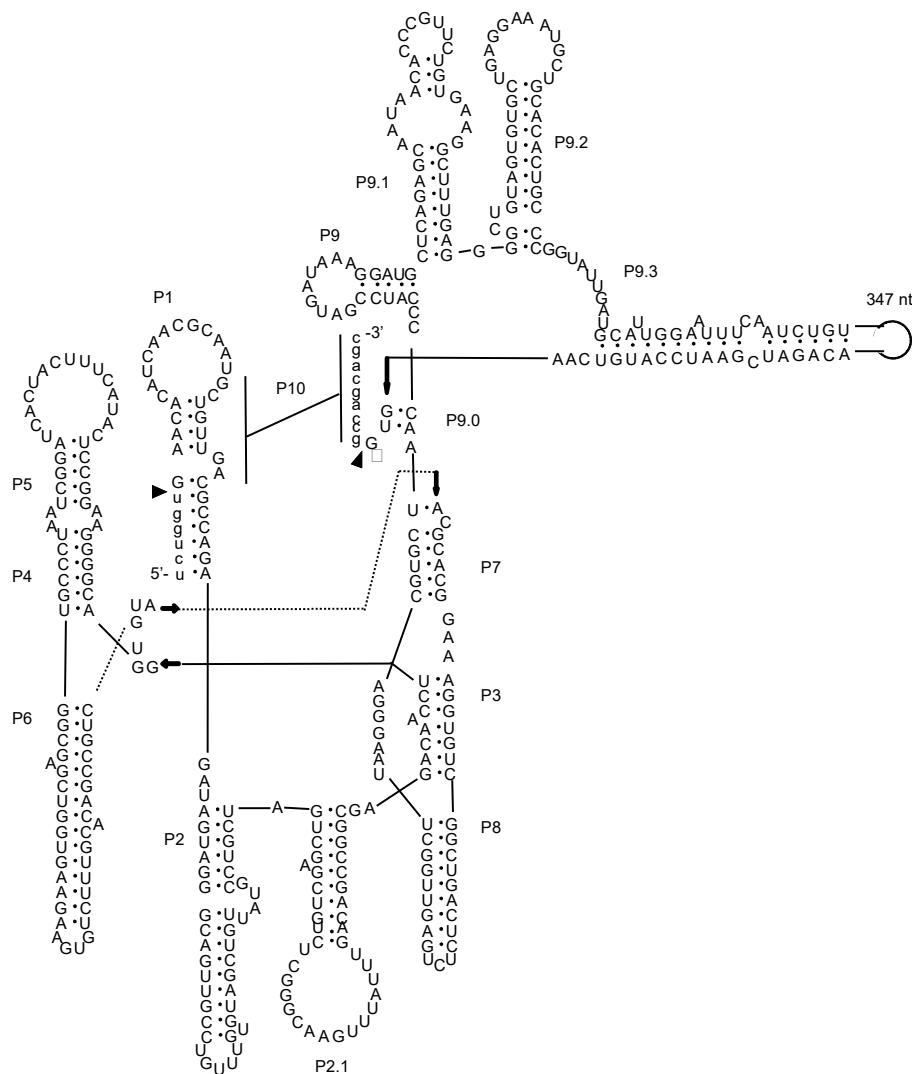


**Figure 1.** Predicted secondary structure of the group I intron S516 of *Desmodium* sp. *nl3*, located in the 18S rDNA. Paired elements are indicated as P1 to P9, the intron sequence is in upper case letters, the exon sequence in lower case letters.

### 3.3. Microalgal Growth

The morphology of both isolates was observed under the microscope. Cells of *Desmodium* sp. *nl3* are oval-shaped with a diameter ranging between 6 and 10  $\mu\text{M}$  while cells of *N. salina* *nl6* are smaller, with a diameter ranging between 3 and 5  $\mu\text{M}$ . F/2 medium was utilized for the investigation of the growth of *N. salina* *nl6* (Figure 3a–c). A salinity of 24‰ representing the average salinity found in the shrimp ponds where the microalgal sample has been collected was chosen. The temperature was 25 °C and the light intensity was 200  $\mu\text{mol m}^{-2}\text{s}^{-1}$ . The specific growth rate of *nl6* was 0.13  $\text{day}^{-1}$  and the biomass yield was  $0.39 \pm 0.01 \text{ g L}^{-1}$  at the entry of the stationary phase. The specific growth rate of *nl6* was 0.13  $\text{day}^{-1}$  and the biomass yield was  $0.39 \pm 0.01 \text{ g L}^{-1}$  at the entry of the stationary phase. The specific growth rate was consistent with that reported for other *Nannochloropsis* isolates (from 0.073 to 0.21  $\text{day}^{-1}$ ) and was lower than that of *N. salina* CCMP537 and CCMP1176 (0.19  $\text{day}^{-1}$ ) [29], probably because 2% (*v/v*)  $\text{CO}_2$  was supplemented in the F/2 medium for these last two strains. We noticed a change in color during cultivation, from green in lag and exponential phases to yellowish in stationary phase. This phenomenon was also reported by [30,31]. This color change is even more obvious when cells are cultivated on agar plates (Figure 3b,c) where the cells turn orange.

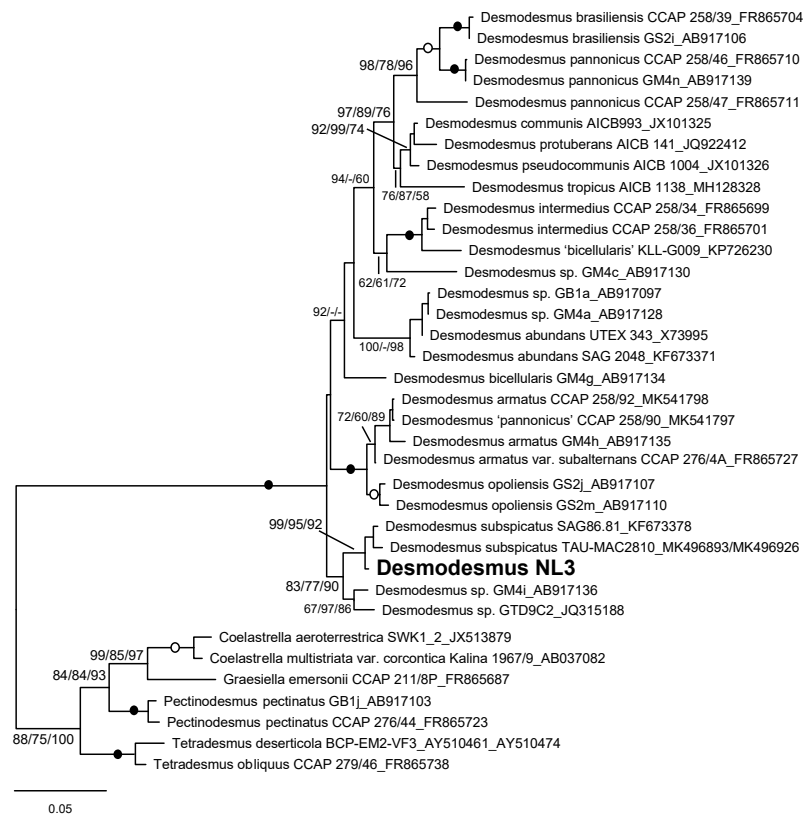


**Figure 2.** Phylogenetic position of isolate n13 within Scenedesmaceae. The phylogenetic tree was built on a selected set of microalgal rDNA (18S–ITS1–5.8S–ITS2) sequences available in GenBank, using maximum likelihood (ML), neighbor-joining (NJ) and maximum parsimony (MP). Bootstrap values after 1000 replicates are indicated at nodes for mL/NJ/MP. Filled and open circles indicate 100 or >95% BV support with all methods, respectively; hyphen, node not supported.

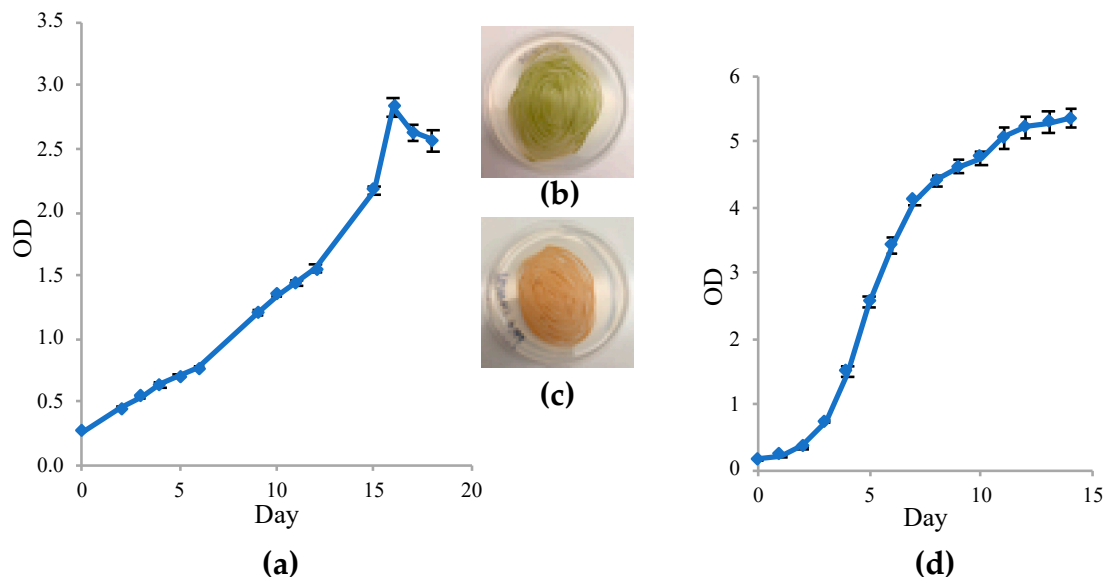


**Figure 3.** Growth curves of the two microalgal isolates. (a) growth curve of *N. salina nl6* in liquid medium ( $n = 3$ , 24‰ NaCl, F/2 medium,  $200 \mu\text{mol m}^{-2}\text{s}^{-1}$ ); (b) Agar plate of *nl6* after 10 days growth; (c) Agar plate of *nl6* after several weeks of growth; (d) growth curve of *Desmodesmus sp. nl3* in liquid medium ( $n = 3$ , TAP medium,  $200 \mu\text{mol m}^{-2}\text{s}^{-1}$ ).

For *nl3*, although the initial isolation was made on F/2 medium (see material and methods), growth was analyzed on Tris-Acetate-Phosphate medium (TAP), which is routinely used for the growth of *Chlamydomonas* [32], a freshwater green microalga belonging to the same class (Chlorophyceae) because *nl3* easily grows on this medium. As shown in Figure 3d, *nl3* had a two-day lag phase before entering the exponential phase from day 3 to day 12. The specific growth rate of *nl3* was  $0.27 \text{ day}^{-1}$ . The cells enter the stationary phase at day 14 with biomass yield of  $1.54 \pm 0.06 \text{ g L}^{-1}$ . The biomass yield was higher than those in other studies. For instance, Ji et al., (2013) [33] reported a maximum biomass of  $0.758 \text{ g L}^{-1}$  from *Desmodesmus* sp. EJ15-2 cultivated in optimal condition of  $30 \text{ }^\circ\text{C}$ ,  $98 \mu\text{mol m}^{-2} \text{ s}^{-1}$ , BG11 medium and 14:10 (Light:Dark) for 14 days. In another study, Zhang et al., (2016) reported biomass yields ranging from  $0.520$  to  $0.792 \text{ g L}^{-1}$  in seven different *Desmodesmus* sp. strains cultivated in BG11 and maintained for 19 days at an irradiance of  $80 \mu\text{mol m}^{-2} \text{ s}^{-1}$  and 14:10 (Light:Dark) at  $25 \pm 1 \text{ }^\circ\text{C}$  [34]. These differences are probably due to the presence of acetate in our medium which provides an additional carbon source for growth, besides atmospheric  $\text{CO}_2$ .

#### 3.4. Pigment Content in the Exponential and Stationary Phases

We then evaluated the pigment content of both strains in mid-exponential and early stationary phase (Table 2). As expected, chlorophyll b is lacking in *N. salina nl6*, as the *Nannochloropsis* genus lacks this type of chlorophyll [35] while it is present in *Desmodesmus* sp. *nl3* which belongs to Chlorophyta. In both strains, most of the pigments decrease upon stationary phase, especially chlorophyll a as already observed in *N. oceanica* [36] and other microalgae [37]. Solovchenko et al., (2014) [36] propose that this is an indication of a down-sizing and a remodeling of the light harvesting antenna of the microalga following nutrient stress. On the contrary, astaxanthin ( $0.36 \pm 0.03 \text{ mg/g DW}$ ) and canthaxanthin ( $0.18 \pm 0.01 \text{ mg/g DW}$ ), two pigments of potential for commercial success [8,38] are detected in the stationary phase of *N. salina nl6*. The content of astaxanthin measured is comparable to that reported in [39] when expressed to the amount of chlorophyll a (2.9% in our case and 2.6% in their case). Associated with the decrease of chlorophyll a, the presence of astaxanthin explains the color change occurring between the exponential and the stationary phase in *N. salina nl6*. When pigment analysis is made on agar plates maintained for several weeks in the light as depicted in Figure 3c, higher amounts of astaxanthin ( $2.52 \pm 1.3 \text{ mg/g DW}$ ) are present, although far less than the amounts obtained for the green alga *Haematococcus pluvialis* ( $8\text{--}36 \text{ mg/g DW}$ ) [40], the well-known astaxanthin producer. Nevertheless, these latter results suggest that astaxanthin production could be optimized in *N. salina nl6*.

On the other hand, lutein is detected in *Desmodesmus* sp. *nl3* and the amount does not vary significantly between exponential ( $1.88 \pm 0.11 \text{ mg DW}$ ) and stationary ( $1.63 \pm 0.24 \text{ mg DW}$ ) phase (Table 2). This amount is in the range of that found in *Scenedesmus obliquus*, a green microalga of the same family [41]. In addition, as it is shown that the lutein content may vary upon various stresses [42], we cultivated *Desmodesmus* sp. *nl3* under various salinities (between 10 and 35‰) (Table 2). We noticed a significant increase of the lutein content upon salt addition, with the 20‰ salinity showing the highest lutein content ( $7.00 \pm 0.24 \text{ mg/g}$ ) at the beginning of the stationary phase. The biomass yield does not change much in the different salinity conditions (Table 2), meaning that the lutein content reaches  $9.87 \text{ mg L}^{-1}$  in 20‰ salinity against  $2.51 \text{ mg L}^{-1}$  when cells are cultivated in fresh water medium. The photoprotective mechanisms in the presence of salt and light which are activated to avoid the presence of reactive oxygen species will be worthy to study, knowing that differences exist inside Chlorophyta [43]. The protein content was determined in the different salinities tested and shown to represent around 40% of the DW (Table 2).



**Table 2.** Pigment content in exponential and stationary phase (mg/g DW). *N. salina nl6* was cultivated in F/2 medium (24‰ salinity) and *Desmodesmus sp. nl3* on TAP medium; Lutein, protein, and biomass contents of *Desmodesmus sp. nl3* (n = 3).

Pigment	<i>N. salina nl6</i>		<i>Desmodesmus sp. nl3</i>		
	Exponential Phase	Stationary Phase	Exponential Phase	Stationary Phase	
Lutein	0.48 ± 0.02	0.22 ± 0.03	1.88 ± 0.11	1.63 ± 0.24	
Neoxanthin	0.13 ± 0.00	nd	0.16 ± 0.02	0.13 ± 0.08	
Violaxanthin	2.51 ± 0.11	0.59 ± 0.10	0.61 ± 0.05	0.31 ± 0.07	
Antheraxanthin	nd	nd	nd	0.13 ± 0.03	
Chlorophyll b	-	-	3.79 ± 0.45	2.16 ± 0.09	
Chlorophyll a	12.20 ± 0.49	3.07 ± 0.36	14.16 ± 0.64	6.82 ± 0.33	
Beta-carotene	0.27 ± 0.00	0.06 ± 0.01	0.52 ± 0.05	0.18 ± 0.02	
Astaxanthin	nd	0.36 ± 0.03	nd	nd	
Canthaxanthin	nd	0.18 ± 0.01	0.02 ± 0.00	0.01 ± 0.00	
<i>Desmodesmus sp. nl3</i> (Stationary Phase)	Salinity				
	0‰	10‰	20‰	30‰	35‰
Lutein	1.63 ± 0.24	4.01 ± 0.55	7.00 ± 0.24	5.67 ± 0.17	2.24 ± 0.72
Protein (% DW)	26.3 ± 1.99	40.54 ± 2.96	38.07 ± 0.29	39.26 ± 1.71	31.93 ± 2.55
Biomass yield (g L <sup>-1</sup> )	1.54 ± 0.06	1.19 ± 0.04	1.41 ± 0.03	1.21 ± 0.02	1.12 ± 0.00

### 3.5. Fatty Acid Profile and Content in the Exponential and Stationary Phases

We then examined the fatty acid profile and content in exponential and onset of the stationary phase in *N. salina nl6* and *Desmodesmus sp. nl3* in the growth conditions mentioned above (F/2 medium and 24‰ salinity for *N. salina nl6* and TAP medium for *Desmodesmus sp. nl3*). As indicated in Table 3 (left), *N. salina nl6* fatty acid content is 18.87 ± 3.21% of DW in exponential phase and reaches 40.41 ± 2.87 of DW in stationary phase, indicating that this strain is a bona fide oleaginous microalga. The fatty acid profile is typical of *Nannochloropsis* species, and characterized by four main fatty acids: palmitic (16:0), palmitoleic (16:1n-7), arachidonic (20:4n-6) and eicosapentaenoic (20:5n-3) (EPA) acids [44].

**Table 3.** Fatty acid profiles of *N. salina nl6* (F/2 medium 24‰ salinity) and *Desmodesmus sp. nl3* (TAP medium) in exponential and stationary phases (n = 3).

Fatty Acid	<i>N. salina nl6</i>		<i>Desmodesmus sp. nl3</i>	
	Exponential Phase	Stationary Phase	Exponential Phase	Stationary Phase
C <sub>14</sub>	nd	0.68 ± 0.21	nd	nd
C <sub>16</sub>	55.75 ± 1.86	44.62 ± 1.39	24.81 ± 0.62	25.70 ± 1.75
C <sub>16:1</sub> (C16:1n-7)	35.64 ± 2.15	33.61 ± 1.24	nd	nd
C <sub>18</sub>	nd	1.28 ± 0.56	1.60 ± 0.81	nd
C <sub>18:1-cis</sub>	2.79 ± 0.86	7.07 ± 0.78	12.12 ± 0.95	27.73 ± 1.27
C <sub>18:2-cis</sub>	nd	0.65 ± 0.24	11.20 ± 0.81	21.74 ± 0.41
C <sub>18:3(cis-Δ9,12,15)</sub>	-	-	50.27 ± 0.32	24.83 ± 2.20
C <sub>20:3</sub> (C20:3n-6)	1.01 ± 0.42	1.11 ± 0.15	-	-
C <sub>20:4</sub> (C20:4n-6)	0.42 ± 0.28	4.01 ± 0.29	-	-
C <sub>20:5</sub> (C20:5n-3)	4.39 ± 0.73	7.08 ± 0.39	-	-
Σ SFA <sup>a</sup>	55.75 ± 1.86	46.47 ± 1.20	26.41 ± 1.43	25.70 ± 1.75
Σ MUFA <sup>b</sup>	38.43 ± 1.60	40.68 ± 1.00	12.12 ± 0.95	27.73 ± 1.27
Σ PUFA <sup>c</sup>	5.82 ± 1.33	12.86 ± 0.95	61.47 ± 0.48	46.57 ± 2.44
% DW	18.87 ± 3.21	40.41 ± 2.87	10.22 ± 0.91	8.65 ± 0.50

<sup>a</sup> SFA: saturated fatty acids, <sup>b</sup> MUFA: monounsaturated fatty acids, <sup>c</sup> PUFA: polyunsaturated fatty acids.

The total fatty acid content of *Desmodesmus sp. nl3* is around 10% DW (Table 3 right), which is expected since green microalgae are not considered as oleaginous. The fatty acid profile is typical of

green microalgae, with C16:0 and C18:3 as main fatty acids [45]. The chain lengths are between C<sub>14</sub> and C<sub>18</sub>, as commonly found in members of Chlorophyta [46].

We then investigated whether these strains would present similar fatty acid profiles in other growth conditions (Tables 4 and 5). For that purpose, we cultivated microalgal cells at different salinities, 10‰, 20‰, 30‰, and 35‰, and harvested at the onset of the stationary phase. Across the four salinity conditions, fatty acid profiles of both strains varied slightly. The biomass yields do not vary much either (see Table 4 for *N. salina nl6* and Table 2 for *Desmodesmus* sp. *nl3*).

**Table 4.** Fatty acid profiles of *N. salina nl6* in different salinities (n = 2) harvested in stationary phase.

<i>N. salina nl6</i>	Salinity			
	10‰	20‰	30‰	35‰
Fatty Acid				
C <sub>14</sub>	2.81 ± 0.03	2.90 ± 0.01	3.89 ± 0.09	1.94 ± 0.51
C <sub>16</sub>	48.50 ± 5.25	43.85 ± 2.14	43.86 ± 0.59	44.41 ± 1.35
C <sub>16:1</sub> (C16:1n-7)	40.06 ± 3.99	38.25 ± 1.01	36.37 ± 0.82	37.59 ± 1.58
C <sub>18</sub>	nd	1.52 ± 0.83	1.24 ± 0.36	0.63 ± 0.16
C <sub>18:1-cis</sub>	8.63 ± 1.28	11.25 ± 0.63	10.88 ± 1.10	10.89 ± 0.29
C <sub>18:2-cis</sub>	nd	0.40 ± 0.04	0.57 ± 0.09	0.18 ± 0.25
C <sub>20</sub>	nd	nd	nd	nd
C <sub>20:3</sub> (C20:3n-6)	nd	nd	nd	0.01 ± 0.00
C <sub>20:4</sub> (C20:4n-6)	nd	0.97 ± 0.09	1.51 ± 0.38	1.93 ± 0.24
C <sub>20:5</sub> (C20:5n-3)	nd	0.86 ± 0.19	1.68 ± 0.47	2.44 ± 0.31
Σ SFA <sup>a</sup>	51.31 ± 5.28	48.27 ± 1.31	48.99 ± 1.04	46.98 ± 1.00
Σ MUFA <sup>b</sup>	48.69 ± 5.28	49.50 ± 1.65	47.26 ± 0.28	48.47 ± 1.30
Σ PUFA <sup>c</sup>	nd	2.23 ± 0.33	3.76 ± 0.76	4.55 ± 0.29
Biomass yield (g/L)	0.4 ± 0.01	0.44 ± 0.00	0.49 ± 0.00	0.48 ± 0.03

<sup>a</sup> SFA: saturated fatty acids; <sup>b</sup> MUFA: monounsaturated fatty acids; <sup>c</sup> PUFA: polyunsaturated fatty acids.

**Table 5.** Fatty acid profiles of *Desmodesmus* sp. *nl3* in different salinities (n = 3) harvested in stationary phase.

<i>Desmodesmus</i> sp. <i>nl3</i>	Salinity			
	10‰	20‰	30‰	35‰
% Fatty Acids				
C <sub>14</sub>	nd	nd	nd	nd
C <sub>16</sub>	19.00 ± 0.33	17.54 ± 1.95	18.05 ± 0.63	21.53 ± 0.51
C <sub>16:1</sub>	nd	nd	1.51 ± 0.27	3.62 ± 0.36
C <sub>18</sub>	nd	nd	nd	0.55 ± 0.54
C <sub>18:1-cis</sub>	9.47 ± 0.97	6.04 ± 0.21	14.64 ± 0.51	26.23 ± 2.69
C <sub>18:2-cis</sub>	27.70 ± 0.89	22.71 ± 1.01	23.60 ± 1.24	19.22 ± 0.47
C <sub>18:3(cis-Δ9,12,15)</sub>	43.83 ± 1.79	53.71 ± 2.35	42.20 ± 0.78	29.03 ± 3.79
Σ SFA <sup>a</sup>	19.00 ± 0.33	17.54 ± 1.95	18.05 ± 0.63	21.90 ± 0.93
Σ MUFA <sup>b</sup>	9.47 ± 0.97	6.04 ± 0.21	16.14 ± 0.43	29.85 ± 2.85
Σ PUFA <sup>c</sup>	71.53 ± 1.30	76.42 ± 1.76	65.80 ± 0.58	48.26 ± 3.78

<sup>a</sup> SFA: saturated fatty acids; <sup>b</sup> MUFA: monounsaturated fatty acids; <sup>c</sup> PUFA: polyunsaturated fatty acids.

### 3.6. Effect of Salinity Conditions on Biodiesel Quality

The potential of the microalgal oils of both strains for biodiesel production was investigated by calculating seven biodiesel properties: average degree of unsaturation (ADU), kinematic viscosity (kV, 40 °C, mm<sup>2</sup> s<sup>-1</sup>), specific gravity (SG, kg L<sup>-1</sup>), cloud point (CP, °C), cetane number (CN), iodine value (IV, g I<sub>2</sub> 100g<sup>-1</sup>), and higher heating value (HHV, (Mj kg<sup>-1</sup>)) (see Materials and Methods) based on the fatty acid contents and profiles (Tables 6 and 7). Those properties were evaluated through the comparison with the US (ASTMD 6751-08) and Europe (EN 14214) biodiesel standards. As depicted in these tables, all the six values agreed with the requirements of the two standards for *N. salina nl6* while iodine parameter (IV) did not for *Desmodesmus* sp. *nl3*.

**Table 6.** Biodiesel properties of *N. salina nl6* in different salinities and growth phases.

Biodiesel Properties	Salinity (Stationary Phase)				Stationary Phase	Exponential Phase	Standards	
	10‰	20‰	30‰	35‰	24‰	24‰	US (ASTMD 6751-08)	Europe (EN 14214)
ADU	0.49 ± 0.05	0.58 ± 0.00	0.63 ± 0.04	0.69 ± 0.01	0.97 ± 0.04	0.65 ± 0.06	-	-
kV	4.90 ± 0.03	4.84 ± 0.00	4.81 ± 0.03	4.77 ± 0.00	4.6 ± 0.02	4.8 ± 0.04	1.9–6.0	3.5–5.5
SG	0.88 ± 0.00	0.88 ± 0.00	0.88 ± 0.00	0.88 ± 0.00	0.88 ± 0.00	0.88 ± 0.00	0.85–0.9	-
CP (°C)	13.49 ± 0.70	12.18 ± 0.03	11.60 ± 0.53	10.81 ± 0.09	7.07 ± 0.47	11.3 ± 0.74	-	-
CN	59.63 ± 0.35	58.98 ± 0.01	58.69 ± 0.26	58.29 ± 0.05	56.42 ± 0.24	58.54 ± 0.37	min 47	min 51
IV	48.93 ± 3.92	56.20 ± 0.15	59.45 ± 2.95	63.83 ± 0.51	84.68 ± 2.64	61.12 ± 4.13	-	Max 120
HHV	39.39 ± 0.09	39.56 ± 0.00	39.64 ± 0.07	39.74 ± 0.01	40.24 ± 0.06	39.68 ± 0.10	-	-

**Table 7.** Biodiesel properties of *Desmodesmus* sp. *nl3* in different salinities and growth phases.

Biodiesel Properties	Salinity (Stationary Phase)				Stationary Phase	Exponential Phase	Standards	
	10‰	20‰	30‰	35‰	0‰	0‰	US (ASTMD 6751-08)	Europe (EN 14214)
ADU	1.96 ± 0.03	2.13 ± 0.06	1.90 ± 0.01	1.55 ± 0.08	1.46 ± 0.06	1.85 ± 0.02	-	-
kV	3.97 ± 0.02	3.86 ± 0.04	4.01 ± 0.01	4.23 ± 0.05	4.29 ± 0.04	4.04 ± 0.01	1.9–6.0	3.5–5.5
SG	0.88 ± 0.00	0.88 ± 0.00	0.88 ± 0.00	0.88 ± 0.00	0.88 ± 0.00	0.88 ± 0.0	0.85–0.9	-
CP (°C)	-6.23 ± 0.44	-8.40 ± 0.79	-5.38 ± 0.15	-0.76 ± 1.13	0.54 ± 0.83	-4.76 ± 0.21	-	-
CN	49.78 ± 0.22	48.70 ± 0.39	50.21 ± 0.08	52.51 ± 0.57	53.16 ± 0.42	50.52 ± 0.11	min 47	min 51
IV	158.74 ± 2.47	170.81 ± 4.40	153.97 ± 0.86	128.27 ± 6.31	121.06 ± 4.65	150.53 ± 1.19	-	Max 120
HHV	41.99 ± 0.06	42.28 ± 0.10	41.88 ± 0.02	41.27 ± 0.15	41.10 ± 0.11	41.80 ± 0.03	-	-

#### 4. Discussion

In this study, two microalgal isolates from the Ninh Thuan province of Vietnam have been genetically identified and characterized in terms of growth at lab-scale and biomass composition.

The *nl6* isolate is identical to *N. salina* D12 recorded in GenBank (JX185299.1) based on 18S rDNA–ITS sequence. The strain exhibits a high percentage of fatty acids at the beginning of the stationary phase (40% DW), and a high percentage of saturated fatty acids (i.e., 46% of SFA), suggesting *nl6* as a promising candidate for biodiesel production. In addition, there is also a high proportion of MUFAs (nearly 50%), which is an important index for the evaluation of biodiesel quality [29,47]. Indeed, in biodiesel, oxidative stability is improved by saturated fatty esters due to their high cetane number while low-temperature properties are favored by unsaturated fatty esters [48]. Amongst these MUFAs, besides its role in biodiesel, palmitoleic acid (C16:1), which represents 30–40% of the total fatty acids has generated attention in recent years due to its nutritional value [49], and its use in the production of linear low-density polyethylene [50]. Concerning PUFAS, and as quite well known for long time, EPA is also interesting for human health and represents between 4 and 7% of the total fatty acids, which is in the range observed for this genus [51]. Pigment investigations also outlined a substantial increase of astaxanthin and canthaxanthin in stationary phase. Therefore, this microalga is attractive both for biodiesel, and its nutritional value, which makes it appreciated in aquaculture. The fact that the fatty acid profile does not change much in a large range of salinity (10–35‰) makes this isolate particularly attractive for cultivation in open ponds close to the sea in tropical climates where heavy rains during monsoon are responsible for fluctuating salinities. The disadvantage we observe here concerns its low specific growth rate which should be improved to make the strain economically competitive.

The *nl3* isolate belongs to the *Desmodesmus* genus and phylogenetic analysis based on the 18S rDNA–ITS sequence shows that the strain groups with *D. subspicatus*. The strain has two group I introns, one S516 and S1046. The S516 group I intron was shown to display a typical secondary structure, which can be assigned to class E. Group I introns are found in organellar genomes of almost all eukaryotes and nuclear rDNA genes of unicellular eukaryotes such as fungi, algae and amoebae [20,52] and are able to self-splice at least in vitro to give the mature RNA sequence. Some of them also have a homing endonuclease (HE) gene that increases their ability to spread [52]. Nearly all the S516 introns of the Scenedesmeaceae family analyzed in our study including that of *Desmodesmus* sp. *nl3* are grouped in the phylogenetic tree based on the conserved P3–P8 structure of the introns (Figure S1a). When considering the entire sequence of the introns excluding endonuclease gene, pairwise similarity analysis suggests that the *nl3* intron is much closer to the introns of *D. intermedius* (71.5% similarity) and *D. opoliensis* GS2m and GS2j (64–67% similarity, respectively), than to that of *Coelastrella* (46.5% similarity) (Figure S1b). In addition, the group I intron of *D. opoliensis* GS2j is longer than all others and has an HE with a His-Cys box domain [36] (Figure S2), suggesting that this intron could be mobile. HEs typically recognize sequences of 18–24 bp in intron-less sequences and introduce a double strand break. The double strand break is then repaired by copying the intron sequence in the intron-less DNA sequence [52]. Interestingly, the HE in the *D. opoliensis* GS2j intron is inserted into P9.3, which is also the branch whose length varies between the analyzed introns. Available data suggest that the introns in the algae studied here may have a common origin, subsequently either persisting (*D. opoliensis* GS2j) or changing with the degradation (*D. intermedius*, *D. opoliensis* GS2m, *Desmodesmus* sp. *nl3*) and final loss of HE (*Desmodesmus* GM4i), and the intron itself, consistent with the homing life cycle of invasion and loss of the introns in closely related species [53].

The biodiesel properties of the fatty acids of *Desmodesmus* sp. *nl3* do not match with the US and European standards because of the iodine value. However, this strain has other interesting characteristics, such as its high lutein content, which, coupled to its high protein content, makes it attractive for the fish industry since lutein supplementation (50 mg kg<sup>-1</sup>) improves survival and promotes efficient carotenoid pigmentation of the skin of goldfish juveniles [54]. In addition, C18:3 ( $\alpha$ -linolenic acid), represents between 40 and 50% of the total fatty acid content in nearly all the tested conditions. This fatty acid is usually in low amounts in vegetal oils and has also been detected in

substantial amounts in other green microalgal isolates from Vietnam [55]. Like for *N. salina nl6*, the tolerance of *nl3* to various salinities also makes it interesting for cultivation in coastal regions located in tropical climates. In addition, since this strain is able to assimilate organic carbon source like acetate and ammonium as nitrogen source, it is also interesting for combining wastewater remediation and use of the resulting algal biomass for aquaculture and fisheries purposes.

## 5. Conclusions

Our results show the potential of two microalgal isolates for cultivation in coastal regions of Vietnam. *Desmodesmus* sp. *nl3* possesses a group I intron in the 18S rDNA sequence, closely related to other group I introns of the *Desmodesmus* genus. This robust species reaches decent biomass yield with high protein and lutein contents at the beginning of the stationary in lab-scale conditions, tolerates various salinities and is able to assimilate an organic carbon source and ammonium. These characteristics makes it attractive for wastewater treatment coupled to aquaculture purposes. *N. salina nl6* also tolerates various salinities and has an attractive fatty acids profile and content including PUFAs which could be exploited for biodiesel and nutraceutical aspects. The fact that the two strains with contrasting characteristics have been isolated in the same ponds in the Ninh Thuan province of Vietnam reflects the microalgal diversity found in this region, where growth conditions vary greatly in terms of water availability and salinity depending on the season. For outdoor cultivation, future analyses should focus on the tolerance to other stresses such as light intensity and temperature.

**Supplementary Materials:** The following are available online at <http://www.mdpi.com/1996-1073/13/4/898/s1>, Figure S1: Analysis of *Desmodesmus* sp. *nl3* S516 intron. (a) Phylogenetic analysis of S516 group I introns of IE and IC1 classes amongst microalgae based on the P3–P8 conserved structures, (b) pairwise analysis of group I introns of the Scenedesmaceae family. Figure S2: Amino acid sequences of homing endonucleases (HE) of *Naegleria jamiesoni* (Njam, AAB71747.1), *Porphyra umbilicalis* (Pumb, AAV35433), *Allovahlkampfia spelaea* (Aspe, ABD62811), *Coemansia mojavensis* (Cmoj, BAB87243), *Naegleria philippinensis* (Nphil, CAJ44447), *Desmodesmus opoliensis* GS2j (DopS2j, AB917110), *Sclerotinia sclerotiorum* (Sscl, XP\_001587714). Color code (according Clustal X color scheme): blue: hydrophobic residues; red: positively charged residues; magenta: negatively charged residues; green: polar residues; cyan: aromatic residues, orange: glycine residue, yellow: proline residue. See [21] for detailed analysis of HE.

**Author Contributions:** Conceptualization, G.E. and C.R.; Funding acquisition, H.A.L. and G.E.; Methodology, G.E. and C.R.; Supervision, G.E. and C.R.; Validation, T.N.L., Z.A., A.C., D.C., G.E. and C.R.; Writing—original draft, T.N.L.; Writing—review & editing, T.N.L., D.C., H.A.L., G.E. and C.R. All authors have read and agreed to the published version of the manuscript.

**Funding:** The authors wish to thank the Académie de Recherche et d’Enseignement Supérieur (ARES-CCD, Brussels, Belgium) for their financial support in the frame of the RENEWABLE project (REmoval of NutriEnts in Wastewater treatments via microAlgae and Biofuel/biomass production for Environmental sustainability in Vietnam, PRD 2016–2020). A.C. is the recipient of an Action de Recherche Concertée doctoral fellowship from the University of Liege (DARKMET ARC grant 17/21–08).

**Acknowledgments:** The authors wish to thank M. Radoux for expert technical assistance.

**Conflicts of Interest:** The authors declare no conflict of interest.

## References

1. Rodolfi, L.; Chini, G.; Niccol, Z.; Giulia, B.; Natascia, P.; Gimena, B.; Mario, B.; Tredici, R. Microalgae for oil: Strain selection, induction of lipid synthesis and outdoor mass cultivation in a low-cost photobioreactor. *Biotechnol. Bioeng.* **2009**, *102*, 100–112. [[CrossRef](#)] [[PubMed](#)]
2. Sydney, E.B.; Sydney, A.C.N.; de Carvalho, J.C.; Soccol, C.R. Microalgal strain selection for biofuel production. In *Biomass, Biofuels and Biochemicals: Biofuels from Algae*; Panday, A., Chang, J.S., Soccol, C.R., Lee, D.J., Chisti, Y., Elsevier, B.V., Eds.; Elsevier: Amsterdam, The Netherlands, 2019; pp. 59–66.
3. Laurens, L.M.L.; Chen-Glasser, M.; McMillan, J.D. A perspective on renewable bioenergy from photosynthetic algae as feedstock for biofuels and bioproducts. *Algal Res.* **2017**, *24*, 261–264. [[CrossRef](#)]
4. Hu, H.; Gao, K. Optimization of growth and fatty acid composition of a unicellular marine picoplankton, *Nannochloropsis* sp., with enriched carbon sources. *Biotechnol. Lett.* **2003**, *25*, 421–425. [[CrossRef](#)] [[PubMed](#)]

5. Sajjadi, B.; Chen, W.Y.; Raman, A.A.A.; Ibrahim, S. Microalgae lipid and biomass for biofuel production: A comprehensive review on lipid enhancement strategies and their effects on fatty acid composition. *Renew. Sustain. Energy Rev.* **2018**, *97*, 200–232. [[CrossRef](#)]
6. Petrie, J.R.; Singh, S.P. Expanding the docosahexaenoic acid food web for sustainable production: Engineering lower plant pathways into higher plants. *AoB Plants* **2011**, *2011*. [[CrossRef](#)]
7. Spolaore, P.; Joannis-Cassan, C.; Duran, E.; Isambert, A. Commercial applications of microalgae. *J. Biosci. Bioeng.* **2006**, *101*, 87–96. [[CrossRef](#)]
8. Gong, M.; Bassi, A. Carotenoids from microalgae: A review of recent developments. *Biotechnol. Adv.* **2016**, *34*, 1396–1412. [[CrossRef](#)]
9. De Vries, J.; Archibald, J.M. Endosymbiosis: Did Plastids Evolve from a Freshwater Cyanobacterium? *Curr. Biol.* **2017**, *27*, R103–R122. [[CrossRef](#)]
10. De Vries, J.; Gould, S.B. The monoplastidic bottleneck in algae and plant evolution. *J. Cell Sci.* **2018**, *131*, jcs203414. [[CrossRef](#)]
11. Archibald, J.M. Genomic perspectives on the birth and spread of plastids. *Proc. Natl. Acad. Sci. USA* **2015**, *112*, 10147–10153. [[CrossRef](#)]
12. Keeling, P.J. The Number, Speed, and Impact of Plastid Endosymbioses in Eukaryotic Evolution. *Annu. Rev. Plant Biol.* **2013**, *64*, 583–607. [[CrossRef](#)] [[PubMed](#)]
13. Newman, S.M.; Boynton, J.E.; Gillham, N.W.; Randolph-Anderson, B.L.; Johnson, A.M.; Harris, E.H. Transformation of chloroplast ribosomal RNA genes in *Chlamydomonas*: Molecular and genetic characterization of integration events. *Genetics* **1990**, *126*, 875–888. [[PubMed](#)]
14. Harris, E.H. *The Chlamydomonas Sourcebook*; Elsevier Inc.: Amsterdam, The Netherlands, 1989.
15. Guillard, R.R.; Ryther, J.H. Studies of marine planktonic diatoms. I. *Cyclotella nana* Hustedt, and *Detonula confervacea* (Cleve) Gran. *Can. J. Microbiol.* **1962**, *8*, 229–239. [[CrossRef](#)] [[PubMed](#)]
16. Makridis, P.; Vadstein, O. Food size selectivity of *Artemia franciscana* at three. *J. Plankton Res.* **1999**, *21*, 2191–2201. [[CrossRef](#)]
17. Wood, A.M.; Everroad, R.C.; Wingard, L.M. Measuring growth rates in microalgal cultures. In *Algal Culturing Techniques*; Andersen, R.A., Ed.; Elsevier: Amsterdam, The Netherlands, 2005; pp. 269–285.
18. Hoekman, S.K.; Broch, A.; Robbins, C.; Cenicerros, E.; Natarajan, M. Review of biodiesel composition, properties, and specifications. *Renew. Sustain. Energy Rev.* **2012**, *16*, 143–169. [[CrossRef](#)]
19. Bradford, M.M. A rapid and sensitive method for the quantitation of microgram quantities of protein utilizing the principle of protein-dye binding. *Anal. Biochem.* **1976**, *72*, 248–254. [[CrossRef](#)]
20. Wilgenbusch, J.C.; Swofford, D. Inferring Evolutionary Trees with PAUP\*. *Curr. Protoc. Bioinforma.* **2003**. [[CrossRef](#)]
21. Jobb, G.; Von Haeseler, A.; Strimmer, K. TREEFINDER: A powerful graphical analysis environment for molecular phylogenetics. *BMC Evol. Biol.* **2004**, *4*, 18. [[CrossRef](#)]
22. Kumar, S.; Stecher, G.; Tamura, K. MEGA7: Molecular Evolutionary Genetics Analysis Version 7.0 for Bigger Datasets. *Mol. Biol. Evol.* **2016**, *33*, 1870–1874. [[CrossRef](#)]
23. White, T.J.; Bruns, T.; Lee, S.; Taylor, J. *Amplification and Direct Sequencing of Fungal Ribosomal RNA Genes for Phylogenetics: PCR—Protocols and Applications—A Laboratory Manual*; Innis, M.A., Gelfand, D.H., Sninsky, J.J., White, T.J., Eds.; Academic Press Inc.: New York, NY, USA, 1990; ISBN 008088671X.
24. Smolik, M.; Krupa-Malkiewicz, M.; Smolik, B.; Wieczorek, J.; Predygier, K. rDNA variability assessed in PCR reactions of selected accessions of *Acer*. *Not. Bot. Horti Agrobot. Cluj-Napoca* **2011**, *39*, 260–266. [[CrossRef](#)]
25. Hoshina, R. DNA analyses of a private collection of microbial green algae contribute to a better understanding of microbial diversity. *BMC Res. Notes* **2014**, *4*, 792. [[CrossRef](#)] [[PubMed](#)]
26. Suh, S.O.; Jones, K.G.; Blackwell, M. A Group I intron in the nuclear small subunit rRNA gene of *Cryptendoxyla hypophloia*, an ascomycetous fungus: Evidence for a new major class of Group I introns. *J. Mol. Evol.* **1999**, *48*, 493–500. [[CrossRef](#)] [[PubMed](#)]
27. Ma, Y.; Wang, Z.; Yu, C.; Yin, Y.; Zhou, G. Evaluation of the potential of 9 *Nannochloropsis* strains for biodiesel production. *Bioresour. Technol.* **2014**, *167*, 503–509. [[CrossRef](#)] [[PubMed](#)]
28. Hu, Q.; Xiang, W.; Dai, S.; Li, T.; Yang, F.; Jia, Q.; Wang, G.; Wu, H. The influence of cultivation period on growth and biodiesel properties of microalga *Nannochloropsis gaditana* 1049. *Bioresour. Technol.* **2015**, *192*, 157–164. [[CrossRef](#)] [[PubMed](#)]

29. Wu, Z.; Zhu, Y.; Huang, W.; Zhang, C.; Li, T.; Zhang, Y.; Li, A. Evaluation of flocculation induced by pH increase for harvesting microalgae and reuse of flocculated medium. *Bioresour. Technol.* **2012**, *110*, 496–502. [[CrossRef](#)]
30. Harris, E.H. Chlamydomonas as a model organism. *Annu. Rev. Plant Physiol. Plant Mol. Biol.* **2001**, *52*, 363–406. [[CrossRef](#)]
31. Ji, F.; Hao, R.; Liu, Y.; Li, G.; Zhou, Y.; Dong, R. Isolation of a novel microalgae strain *Desmodesmus* sp. and optimization of environmental factors for its biomass production. *Bioresour. Technol.* **2013**, *148*, 249–254. [[CrossRef](#)]
32. Zhang, Y.; He, M.; Zou, S.; Fei, C.; Yan, Y.; Zheng, S.; Rajper, A.A.; Wang, C. Breeding of high biomass and lipid producing *Desmodesmus* sp. by Ethylmethane sulfonate-induced mutation. *Bioresour. Technol.* **2016**, *207*, 268–275. [[CrossRef](#)]
33. Vieler, A.; Wu, G.; Tsai, C.H.; Bullard, B.; Cornish, A.J.; Harvey, C.; Reca, I.B.; Thornburg, C.; Achawanantakun, R.; Buehl, C.J.; et al. Genome, Functional Gene Annotation, and Nuclear Transformation of the Heterokont Oleaginous Alga *Nannochloropsis oceanica* CCMP1779. *PLoS Genet.* **2012**, *8*, e1003064. [[CrossRef](#)]
34. Solovchenko, A.; Lukyanov, A.; Solovchenko, O.; Didi-Cohen, S.; Boussiba, S.; Khozin-Goldberg, I. Interactive effects of salinity, high light, and nitrogen starvation on fatty acid and carotenoid profiles in *Nannochloropsis oceanica* CCALA 804. *Eur. J. Lipid Sci. Technol.* **2014**, *116*, 635–644. [[CrossRef](#)]
35. Ruivo, M.; Amorim, A.; Cartaxana, P. Effects of growth phase and irradiance on phytoplankton pigment ratios: Implications for chemotaxonomy in coastal waters. *J. Plankton Res.* **2011**, *33*, 1012–1022. [[CrossRef](#)]
36. Hu, J.; Nagarajan, D.; Zhang, Q.; Chang, J.S.; Lee, D.J. Heterotrophic cultivation of microalgae for pigment production: A review. *Biotechnol. Adv.* **2018**, *36*, 54–67. [[CrossRef](#)]
37. Lubian, L.M.; Montero, O.; Moreno-Garrido, I.; Huertas, I.E.; Sobrino, C.; Gonzalez-Del Valle, M.; Pares, G. *Nannochloropsis* (Eustigmatophyceae) as source of commercially valuable pigments. *J. Appl. Phycol.* **2000**, *12*, 249–255. [[CrossRef](#)]
38. Liu, J.; Sun, Z.; Gerken, H.; Liu, Z.; Jiang, Y.; Chen, F. *Chlorella zofingiensis* as an alternative microalgal producer of astaxanthin: Biology and industrial potential. *Mar. Drugs* **2014**, *12*, 3487–3515. [[CrossRef](#)]
39. Chen, W.-C.; Hsu, Y.-C.; Chang, J.-S.; Ho, S.-H.; Wang, L.-F.; Wei, Y.-H. Enhancing production of lutein by a mixotrophic cultivation system using microalga *Scenedesmus obliquus* CWL-1. *Bioresour. Technol.* **2019**, *291*, 121891. [[CrossRef](#)] [[PubMed](#)]
40. Rauytanapanit, M.; Janchot, K.; Kusolkumbot, P.; Sirisattha, S.; Waditee-Sirisattha, R.; Praneenararat, T. Nutrient deprivation-associated changes in green microalga *Coelastrum* sp. TISTR 9501RE enhanced potent antioxidant carotenoids. *Mar. Drugs* **2019**, *17*, 328. [[CrossRef](#)] [[PubMed](#)]
41. Christa, G.; Cruz, S.; Jahns, P.; de Vries, J.; Cartaxana, P.; Esteves, A.C.; Serôdio, J.; Gould, S.B. Photoprotection in a monophyletic branch of chlorophyte algae is independent of energy-dependent quenching (qE). *New Phytol.* **2017**, *214*, 1132–1144. [[CrossRef](#)] [[PubMed](#)]
42. Khozin-Goldberg, I.; Boussiba, S. Concerns over the reporting of inconsistent data on fatty acid composition for microalgae of the genus *Nannochloropsis* (Eustigmatophyceae). *J. Appl. Phycol.* **2011**, *23*, 933–934. [[CrossRef](#)]
43. Plancke, C.; Vigeolas, H.; Höhner, R.; Roberty, S.; Emonds-Alt, B.; Larosa, V.; Willamme, R.; Duby, F.; Onga Dhali, D.; Thonart, P.; et al. Lack of isocitrate lyase in *Chlamydomonas* leads to changes in carbon metabolism and in the response to oxidative stress under mixotrophic growth. *Plant J.* **2014**, *77*, 404–417. [[CrossRef](#)]
44. Lang, I.; Hodac, L.; Friedl, T.; Feussner, I. Fatty acid profiles and their distribution patterns in microalgae: A comprehensive analysis of more than 2000 strains from the SAG culture collection. *BMC Plant Biol.* **2011**, *11*, 124. [[CrossRef](#)]
45. Knothe, G. Improving biodiesel fuel properties by modifying fatty ester composition. *Energy Environ. Sci.* **2009**, *2*, 759–766. [[CrossRef](#)]
46. Ma, X.N.; Chen, T.P.; Yang, B.; Liu, J.; Chen, F. Lipid production from *Nannochloropsis*. *Mar. Drugs* **2016**, *14*, 61. [[CrossRef](#)] [[PubMed](#)]
47. Zhou, W.; Wang, H.; Chen, L.; Cheng, W.; Liu, T. Heterotrophy of filamentous oleaginous microalgae *Tribonema minus* for potential production of lipid and palmitoleic acid. *Bioresour. Technol.* **2017**, *239*, 250–257. [[CrossRef](#)]

48. Wang, H.; Gao, L.; Zhou, W.; Liu, T. Growth and palmitoleic acid accumulation of filamentous oleaginous microalgae *Tribonema minus* at varying temperatures and light regimes. *Bioprocess Biosyst. Eng.* **2016**, *39*, 1589–1595. [[CrossRef](#)]
49. Janssen, J.H.; Wijffels, R.H.; Barbosa, M.J. Lipid Production in *Nannochloropsis gaditana* during Nitrogen Starvation. *Biology* **2019**, *8*, 5. [[CrossRef](#)]
50. Hedberg, A.; Johansen, S.D. Nuclear group I introns in self-splicing and beyond. *Mob. DNA* **2013**, *4*, 17. [[CrossRef](#)]
51. Corsaro, D.; Köhler, M.; Venditti, D.; Rott, M.B.; Walochnik, J. Recovery of an *Acanthamoeba* strain with two group I introns in the nuclear 18S rRNA gene. *Eur. J. Protistol.* **2019**, *68*, 88–98. [[CrossRef](#)]
52. Goddard, M.R.; Burt, A. Recurrent invasion and extinction of a selfish gene. *Proc. Natl. Acad. Sci. USA* **1999**, *96*, 13880–13885. [[CrossRef](#)]
53. Besen, K.P.; Melim, E.W.H.; da Cunha, L.; Favaretto, E.D.; Moreira, M.; Fabregat, T.E.H.P. Lutein as a natural carotenoid source: Effect on growth, survival and skin pigmentation of goldfish juveniles (*Carassius auratus*). *Aquac. Res.* **2019**, *50*, 2200–2206. [[CrossRef](#)]
54. Thao, T.Y.; Linh, D.T.N.; Si, V.C.; Carter, T.W.; Hill, R.T. Isolation and selection of microalgal strains from natural water sources in Viet Nam with potential for edible oil production. *Mar. Drugs* **2017**, *15*, 194. [[CrossRef](#)]
55. Corsaro, D.; Venditti, D. Nuclear Group I introns with homing endonuclease genes in *Acanthamoeba* genotype T4. *Eur. J. Protistol.* **2018**, *66*, 26–35. [[CrossRef](#)] [[PubMed](#)]



© 2020 by the authors. Licensee MDPI, Basel, Switzerland. This article is an open access article distributed under the terms and conditions of the Creative Commons Attribution (CC BY) license (<http://creativecommons.org/licenses/by/4.0/>).